

# Evaluation of Methods to Select Scale Velocities in Icing Scaling Tests

David N. Anderson  
Ohio Aerospace Institute, Brook Park, Ohio

Gary A. Ruff  
Drexel University, Philadelphia, Pennsylvania

## The NASA STI Program Office . . . in Profile

Since its founding, NASA has been dedicated to the advancement of aeronautics and space science. The NASA Scientific and Technical Information (STI) Program Office plays a key part in helping NASA maintain this important role.

The NASA STI Program Office is operated by Langley Research Center, the Lead Center for NASA's scientific and technical information. The NASA STI Program Office provides access to the NASA STI Database, the largest collection of aeronautical and space science STI in the world. The Program Office is also NASA's institutional mechanism for disseminating the results of its research and development activities. These results are published by NASA in the NASA STI Report Series, which includes the following report types:

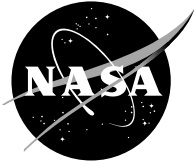
- **TECHNICAL PUBLICATION.** Reports of completed research or a major significant phase of research that present the results of NASA programs and include extensive data or theoretical analysis. Includes compilations of significant scientific and technical data and information deemed to be of continuing reference value. NASA's counterpart of peer-reviewed formal professional papers but has less stringent limitations on manuscript length and extent of graphic presentations.
- **TECHNICAL MEMORANDUM.** Scientific and technical findings that are preliminary or of specialized interest, e.g., quick release reports, working papers, and bibliographies that contain minimal annotation. Does not contain extensive analysis.
- **CONTRACTOR REPORT.** Scientific and technical findings by NASA-sponsored contractors and grantees.

- **CONFERENCE PUBLICATION.** Collected papers from scientific and technical conferences, symposia, seminars, or other meetings sponsored or cosponsored by NASA.
- **SPECIAL PUBLICATION.** Scientific, technical, or historical information from NASA programs, projects, and missions, often concerned with subjects having substantial public interest.
- **TECHNICAL TRANSLATION.** English-language translations of foreign scientific and technical material pertinent to NASA's mission.

Specialized services that complement the STI Program Office's diverse offerings include creating custom thesauri, building customized data bases, organizing and publishing research results . . . even providing videos.

For more information about the NASA STI Program Office, see the following:

- Access the NASA STI Program Home Page at <http://www.sti.nasa.gov>
- E-mail your question via the Internet to [help@sti.nasa.gov](mailto:help@sti.nasa.gov)
- Fax your question to the NASA Access Help Desk at 301-621-0134
- Telephone the NASA Access Help Desk at 301-621-0390
- Write to:  
NASA Access Help Desk  
NASA Center for Aerospace Information  
7121 Standard Drive  
Hanover, MD 21076



# Evaluation of Methods to Select Scale Velocities in Icing Scaling Tests

David N. Anderson  
Ohio Aerospace Institute, Brook Park, Ohio

Gary A. Ruff  
Drexel University, Philadelphia, Pennsylvania

Prepared for the  
37th Aerospace Sciences Meeting and Exhibit  
sponsored by the American Institute of Aeronautics and Astronautics  
Reno, Nevada, January 11-14, 1999

Prepared under Cooperative Agreement NCC3-884

National Aeronautics and  
Space Administration

Glenn Research Center

## Acknowledgments

This work was supported by the NASA Glenn Research Center Icing Branch under grants to the Ohio Aerospace Institute and to Drexel University. The assistance of Alejandro Feo of INTA in providing his thoughts and ideas on scaling is very much appreciated. The untiring help of David Sheldon in overseeing the model preparation in time for these tests was vital to this program. Discussions with Jack Oldenburg and Robert Ide were very helpful in establishing the required spray-bar settings. Finally, the cooperation and assistance of Bill Sexton and the entire IRT staff to install and test the models were, as always, invaluable.

This report contains preliminary findings, subject to revision as analysis proceeds.

The Aerospace Propulsion and Power Program at NASA Glenn Research Center sponsored this work.

Available from

NASA Center for Aerospace Information  
7121 Standard Drive  
Hanover, MD 21076

National Technical Information Service  
5285 Port Royal Road  
Springfield, VA 22100

Available electronically at <http://gltrs.grc.nasa.gov>

# EVALUATION OF METHODS TO SELECT SCALE VELOCITY IN ICING SCALING TESTS

David N. Anderson\*  
Ohio Aerospace Institute  
Brook Park, Ohio 44142

and

Gary A. Ruff†  
Drexel University  
Philadelphia, Pennsylvania 19104

## Abstract

A series of tests were made in the NASA Lewis Icing Research Tunnel to determine how icing scaling results were affected by the choice of scale velocity. Reference tests were performed with a 53.3-cm-chord NACA 0012 airfoil model, while scale tests used a 27.7-cm-chord 0012 model. Tests were made with rime, mixed and glaze ice. Reference test conditions included airspeeds of 67 and 89 m/s, an  $MVD$  of 40  $\mu\text{m}$ , and  $LWC$ s of 0.5 and 0.6  $\text{g}/\text{m}^3$ . Scale test conditions were established by the modified Ruff (AEDC) scaling method with the scale velocity determined in 5 ways. The resulting scale velocities ranged from 85 to 220% of the reference velocity. This paper presents the ice shapes that resulted from those scale tests and compares them to the reference shapes. It was concluded that for freezing fractions greater than 0.8 as well as for a freezing fraction of 0.3, the value of the scale velocity had no effect on how well the scale ice shape simulated the reference shape. For freezing fractions of 0.5 and 0.7, the simulation of the reference shape appeared to improve as the scale velocity increased.

## Nomenclature

$A_c$	Accumulation parameter, dimensionless
$b$	Relative heat factor, dimensionless
$c$	Model chord, m
$h_{film}$	Water-film thickness at leading edge, m
$K_0$	Modified inertia parameter, dimensionless
$LWC$	Cloud liquid-water content, $\text{g}/\text{m}^3$
$M$	Mach number, dimensionless
$MVD$	Water droplet median volume diameter, $\mu\text{m}$
$n$	Freezing fraction, dimensionless
$p_{tot}$	Total pressure, $\text{nt}/\text{m}^2$

\*Senior Research Associate, Member AIAA

† Associate Professor, Associate Fellow AIAA

$p_{st}$	Static pressure, $\text{nt}/\text{m}^2$
$Re$	Reynolds number of model, dimensionless
$Re_\delta$	Reynolds number of water droplet, dimensionless
$t_{st}$	Static temperature, $^\circ\text{C}$
$t_{tot}$	Total temperature, $^\circ\text{C}$
$V$	Air velocity, m/s
$We$	Weber number based on droplet size and water properties, dimensionless
$\phi$	Droplet energy transfer terms in energy balance, $^\circ\text{C}$
$\rho_i$	Ice density, $\text{g}/\text{m}^3$
$\theta$	Air energy transfer terms in energy balance, $^\circ\text{C}$
$\tau$	Accretion time, min

## General Subscripts

$r$	Reference condition
$s$	Scale condition

## Introduction

This paper presents the results of a series of tests recently made in the NASA Lewis Icing Research Tunnel to determine how scaled ice shapes were affected by the choice of scale velocity. Scale velocity was found by applying four physically based methods. A fifth velocity was simply an average of two of the others. One physical method matched the scale and reference values of water-film thickness, one matched the velocity, one, the Weber number and one, the Reynolds number. By establishing which of these approaches was most effective, it was hoped to gain insight into the importance of the physics on which the method was based.

A number of scaling methods have been developed to address the problem of testing models in facilities with limitations in either model size or test conditions. These methods have all been based on a physical description of the ice accretion process with various

assumptions and simplifications. The usual approach in developing a scaling method is to write expressions for the water droplet collection efficiency, total ice accretion on the surface and an energy balance at the stagnation line of the airfoil. The scale and reference values of these expressions are equated to solve for the scale test conditions.

Langmuir and Blodgett<sup>1</sup> defined the modified inertia parameter,  $K_o$ , which is directly related to the local collection efficiency at the stagnation line. This dimensionless parameter has been widely used in scaling methods to insure the scale droplet trajectories, and, thus, collection efficiencies, match the reference. The non-dimensional ice accretion is represented by the accumulation parameter,  $A_c = (LWC V \tau)/(c \rho_i)$ . Heat transfer characteristics can be included by writing the Messinger energy balance<sup>2</sup> in terms of the freezing fraction,  $n$ , the water energy transfer parameter,  $\phi$ , and the air energy transfer parameter,  $\theta$ .  $\phi$  and  $\theta$  are collections of terms in the energy equation that relate to the transfer of energy due to impinging droplets and to airflow over the model, respectively. Ruff<sup>3</sup> performed scale tests with several combinations of these parameters and achieved the best scaling results when all five were matched to the reference values. This approach to scaling is known as the Ruff (or AEDC) Method.

By matching five scaling parameters, the Ruff Method permits the calculation of five scale test conditions from the corresponding reference conditions. They are: static temperature,  $t_{st}$ , cloud water droplet median volume diameter,  $MVD$ , cloud liquid-water content,  $LWC$ , spray duration,  $\tau$ , and test-section total pressure,  $p_{tot}$ . For tunnels, such as the IRT, which do not control the test-section pressure, a modified Ruff Method has been used<sup>4</sup> in which the air-energy transfer parameter,  $\theta$ , is ignored, and the test-section pressure is determined by ambient conditions and test-section velocity.

In the Ruff Method, as with several other scaling methods, the user is free to specify the scale velocity. One way to specify the scale velocity is to equate the scale to the reference velocity. Besides being convenient, this approach insures that  $\theta$  and the Mach number,  $M$ , match the reference values. Other ways to choose the scale velocity can be devised by considering additional physical processes and parameters that may be important in determining ice shape.

In 1986, Olsen and Walker<sup>5</sup> performed tests with close-up photography of the icing surface. This study provided evidence that physics of the surface water might be important in addition to heat transfer in determining the shape of glaze ice. About the same

time, Bilanin<sup>6</sup> published a study of scaling in which he argued that a number of parameters, including the Weber number,  $We$ , and Reynolds number,  $Re$ , need to be considered in formulating scaling methods. Because  $We$  is the ratio of aerodynamic to surface tension forces, it was believed to represent at least some of the surface-water effects and was chosen by Bilanin and Anderson<sup>7,8</sup> to be included in a new scaling method. This constant- $We$  method is in fact the Ruff method with the added restraint that the scale and reference  $We$  match, and from this requirement, the scale velocity can be found. For subscale tests, the constant- $We$  method produces a scale velocity higher than the reference.

A third method is to match the scale and reference  $Re$ , following Bilanin.<sup>6</sup> Because the Reynolds number controls a number of physical processes, including both flow and heat transfer, it is logical that the scale value should be set equal to the reference value. The use of the constant- $Re$  approach in subscale tests produces a scale velocity still higher than that found by matching  $We$ . Although very high scale velocities are rarely practical, the method needs to be evaluated to determine the importance of  $Re$  to ice-accretion scaling.

A method that gives a lower-than-reference scale velocity for subscale models was proposed by Feo.<sup>9</sup> He suggested matching the scale and reference leading-edge water-film thickness, normalized by model size. Feo's water-film thickness was based on a correlation of data taken as part of a study of the effects of rain on

$$\frac{h_{film}}{c} \propto LWC^{1/2} (Re)^{-1/4} (Re_{\delta})^{15/4} (We)^{-9/4}$$

aircraft performance.<sup>10</sup> The best fit was found to be

This correlation was developed from tests with larger water droplets and higher liquid-water contents than those experienced in normal icing encounters. However, in the absence of more relevant data, it can be taken as an approximate representation of the thickness of the water film which forms during glaze ice accretion. The ratio of the scale airspeed to the reference can be found by equating the scale and

$$\frac{V_s}{V_r} = \left( \frac{LWC_s}{LWC_r} \right)^{1/2} \left( \frac{MVD_s}{MVD_r} \right)^{3/2} \left( \frac{c_s}{c_r} \right)^{-1/4}$$

reference non-dimensional water film thickness:

Here it was assumed that the droplet velocity which appears in  $We$  and  $Re_{\delta}$  is proportional to the airspeed, and that differences between scale and reference static pressure and water properties are negligible.

Figure 1 shows typical scale velocities found by the four methods described above for a reference velocity of 67 m/s and for a 1/2-size scale model. A fifth scale velocity is also shown; it is the average of the constant-

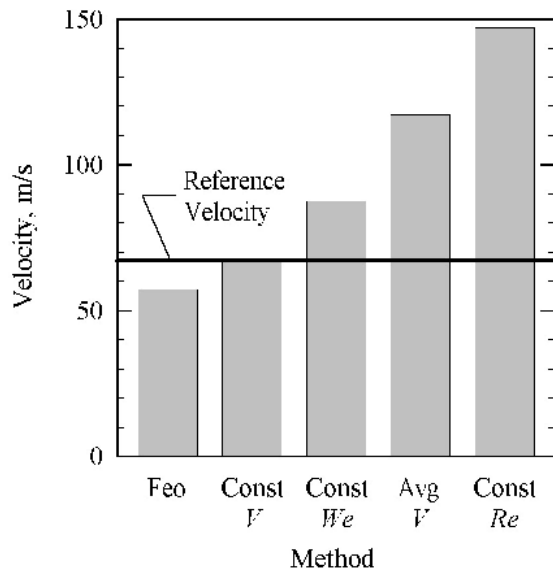


Figure 1. Scale Velocities for 1/2-scale Model. Reference Velocity, 67 m/s.

$We$  and constant- $Re$  velocities. This average- $V$  method has no physical basis, but it can be used as part of a sequence of tests to assist in spotting possible trends with velocity.

In the present study, scaled tests with half-size models were made using the Ruff Method with scale velocity found by each of these five methods.

#### Reference Conditions

Five reference cases with full-size models were chosen for study. These are shown in table I. Case 73

Table I. Reference Test Conditions  
Reference Model: 53.3-cm-Chord NACA 0012

Case	$t_{st}$ , °C	$V$ , m/s	$MVD$ , μm	$LWC$ , g/m <sup>3</sup>	$\tau$ , min	$n$
73	-20.6	89	40	0.5	10.0	1.0
110	-13.9	67	40	0.6	11.2	0.8
111	-11.1	67	40	0.6	11.2	0.7
112	-8.4	67	40	0.6	11.2	0.5
113	-5.6	67	40	0.6	11.2	0.3

produced rime ice, while 110–113 gave mixed or glaze. Cases 110–113 had the same velocity, spray conditions and time, with the temperature increasing from case 110 to case 113 to provide a range of freezing fractions. The reference  $MVD$  and  $LWC$  were selected so that both reference and scale conditions could be tested with the same nozzle set in the IRT. Spray times were chosen to provide the same accumulation parameter for all cases.

#### Test Description

##### NASA Lewis Icing Research Tunnel

Figure 2 is a plan view of the NASA Lewis Icing Research Tunnel (IRT).<sup>11</sup> The IRT has a test section

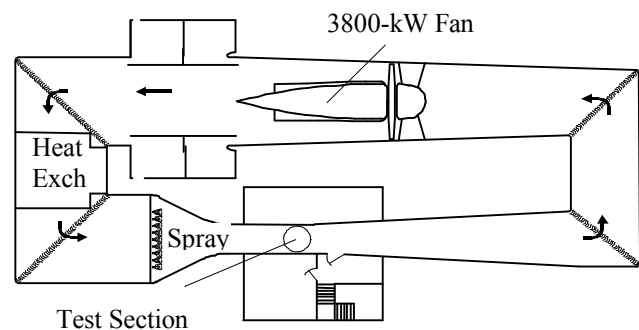


Figure 2. NASA Lewis Icing Research Tunnel (IRT).

width of 2.7 m and a height of 1.8 m. It has a refrigeration system that allows accurate control of the test-section temperature from  $-40$  to  $4^\circ\text{C}$ . A water spray system with ten spray bars simulates the conditions in a natural icing cloud. The test-section cloud droplet size,  $MVD$ , and liquid-water content,  $LWC$ , depend on spray-bar air and water pressures. The relationships among these pressures, the tunnel airspeed and the cloud properties are established periodically by a series of tunnel calibration tests.<sup>12</sup> The cloud has been calibrated over a range of test-section airspeeds from 22 to 156 m/s and droplet median volume diameters from 14 to 50 μm. Two sets of spray nozzles, the Mod-1 and Standard nozzles, are used to provide different ranges of liquid-water content. Depending on the nozzle set, the airspeed and the droplet diameter, the test-section liquid-water content can be controlled from less than 0.2 to over 5 g/m<sup>3</sup>. The Mod-1 nozzles were used for all tests reported here.

#### Test Models and Procedures

Ice accretion was measured on NACA 0012 airfoils with chords of 53.3 cm (reference model) and 26.7 cm

(scale model). Each was mounted vertically, at 0° angle of attack, in the center of the IRT test section. The models were machined from solid aluminum. Both had a span of 61 cm and were placed between end plates as shown in figure 3. The models' mid spans



Figure 3. 53.3-cm-Chord NACA 0012 Model in IRT Test Section.

were located on the tunnel centerline (midway between floor and ceiling of the test section). Five horizontal lines were marked around the leading edge of each airfoil to indicate the location of the mid-span and of positions 2.5 and 5 cm above mid-span and 2.5 and 5 cm below mid-span. Ice shapes were recorded at all but the 5-cm-below-mid-span location. All shapes reported were recorded by hand tracing.

The IRT spray system recirculates water to permit the stabilization of air and water pressures prior to opening the water valve at each nozzle. This feature virtually eliminates start-up transients that were present previously in the IRT. Once the desired temperature and airspeed had been achieved and spray-bar conditions had been set and stabilized, the water valves were opened to initiate the spray, and the spray timer was started. At the completion of the icing spray time, the spray was turned off and the tunnel fan was stopped. Personnel then entered the test section, and a thin heated plate was used to cut horizontal slices into the accreted ice at the desired span-wise locations. The shapes were traced onto cardboard templates and later

digitized for computer storage. Finally, the model was cleaned and the procedure repeated for the next test.

#### Average Test Conditions

Actual reference and scale conditions for the tests reported here are given in table II along with the corresponding scaling parameters. Tunnel and cloud conditions were recorded at 1-sec intervals for tests with the 26.7-cm-chord model and at 2-sec intervals for the 53.3-cm-chord model. Each test condition was also determined from more than one instrument. The total temperature was recorded with eleven type T thermocouples located on the turning vanes just downstream of the heat exchanger. Two pitot-static probes on opposite walls at the entrance to the IRT test section were used to determine test-section velocity. The *MVD* and *LWC* were calculated from the spray-bar air pressure and water-air differential pressure for each of the ten spray bars. The test conditions in Table II have been averaged over the multiple instrument readings as well as over the duration of the spray.

#### Uncertainty in Parameter Values

Typically, the total temperature drifted up and down during each test by about  $\pm 0.1$  °C. Fluctuations in the velocity and the *LWC* on the order of  $\pm 1\%$  were observed, while the droplet size showed little variation after the first 20 sec or so.

Estimates of the uncertainty in the reported conditions were made by considering fluctuations of the values with time, possible instrument errors including calibration, uncertainties in tunnel calibration of *MVD* and *LWC*, and differences in measurements from one location to another. It was concluded that for the conditions of the tests reported here total temperatures are probably known to within  $\pm 1.5$  °C, velocity,  $\pm 2.5\%$ , *MVD*,  $\pm 11\%$  and *LWC*,  $\pm 12\%$ .

#### Results and Discussion

The ice shapes recorded in these tests will be shown with coordinate axes graduated in cm. These axes represent the full-size coordinates of the ice shapes for the reference model. The coordinates for the  $\frac{1}{2}$ -scale shapes were doubled to permit direct comparison with the reference.

Repeatability tests were made to establish typical run-to-run differences in ice shape. Checks of the span-wise ice-shape uniformity were also made, because a highly non-uniform cloud will produce ice shapes which are very sensitive to tracing location.

#### Repeatability of Ice Shapes

Figure 4 presents three comparisons of ice formed on different occasions at the same test conditions and with



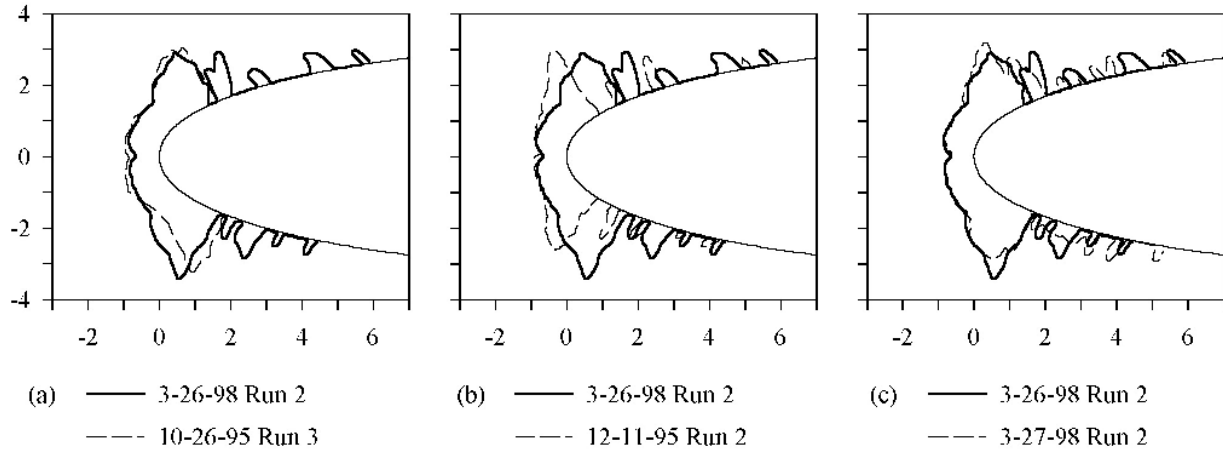


Figure 4. Repeatability of Ice Shapes, 1995–1998. Case 113 Reference at Mid-Span. 53.3-cm-Chord NACA 0012 Airfoil.  $t_{st}$ ,  $-3^{\circ}\text{C}$ ;  $V$ , 67 m/s;  $MVD$ ,  $40\ \mu\text{m}$ ;  $LWC$ ,  $.65\ \text{g/m}^3$ ;  $\tau$ , 11.2 min. Axis Units, cm.

the same 53.3-cm-chord NACA 0012 model. All ice shapes were recorded at the vertical center of the IRT test section. Figure 4(a) compares shapes recorded on 3–26–98 and 10–26–95. The two agree very closely except for some minor differences in the lower horn. This agreement is impressive considering that the tunnel spray bar system had been replaced and recalibrated in 1997. A second comparison is given in figure 4(b) in which the 3–26–98 shape is compared with one from 12–11–95. The latter shape is significantly smaller, and the impingement limits are nearer the leading edge. The final comparison, in figure 4(c), is between the 3–26–98 test and one made the following evening. Again, excellent repeatability of the ice shape is evident. It is clear from these comparisons that the IRT is capable of excellent repeatability even between tests performed years apart. Occasionally, however, test results can vary from one

test entry to another. All scaling results reported here were made during the same tunnel entry to minimize variations of ambient conditions and tunnel characteristics that might influence ice shape.

#### Span-wise Uniformity

Ice shapes recorded at different positions along the model span are shown in figure 5. The mid-span position is at the vertical center of the tunnel test section. Figure 5(a) compares the mid-span shape with the tracing taken 5 cm above the mid-span position. Figure 5(b) compares the mid-span and 2.5 cm above mid-span, and figure 5(c) shows the mid-span shape and one taken 2.5 cm below mid-span. The excellent agreement among the tracings taken at the four positions demonstrates both the consistency of the tracing process and the uniformity of the IRT cloud over at least this limited vertical range. The uniformity

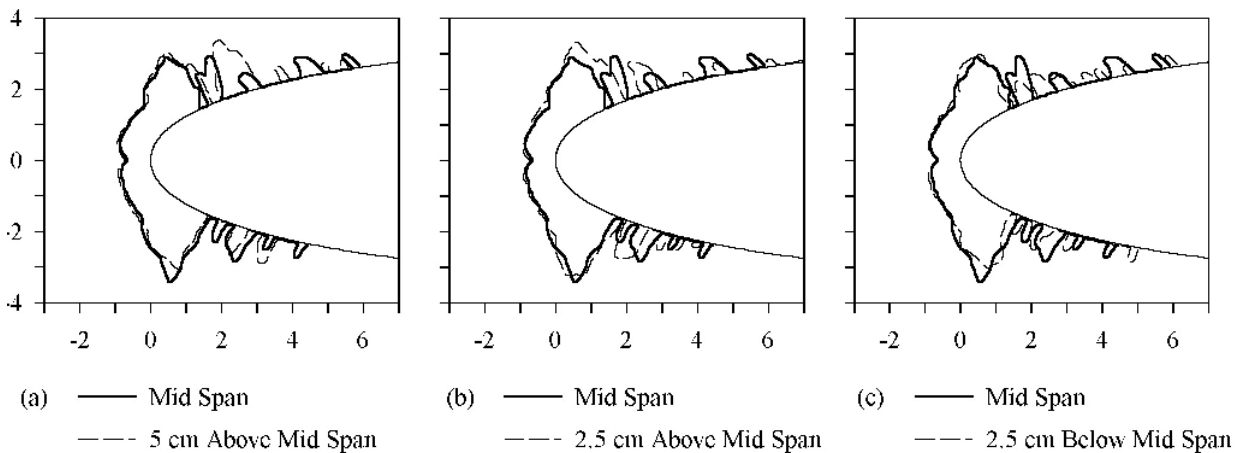


Figure 5. Span-wise Uniformity of Ice Shape. Case 113 Reference, 3–26–98 Run 2. 53.3-cm-Chord NACA 0012 Airfoil.  $t_{st}$ ,  $-3^{\circ}\text{C}$ ;  $V$ , 67 m/s;  $MVD$ ,  $40\ \mu\text{m}$ ;  $LWC$ ,  $.65\ \text{g/m}^3$ ;  $\tau$ , 11.2 min. Axis Units, cm.

indicated by figure 5 was typical of both scale and reference tests for this study. These results gave confidence that scale and reference shape comparisons would not be affected by small errors in tracing location. Scale-to-reference differences in shape reported in the past may sometimes have been due in part to non uniformity in the cloud such that tracings taken at slightly different span-wise locations might have shown better agreement.

### Rime Ice (Case 73)

For rime ice water freezes immediately on impact because convective heat transfer absorbs all the latent heat released on freezing. Consequently, a description of the heat balance at the surface is unnecessary, and, with no liquid water on the ice, dynamics of a liquid surface are irrelevant. Thus, only the accumulation and inertia parameters,  $A_c$  and  $K_0$ , have to be matched between scale and reference, and all of the methods to choose scale velocity should have been equally successful in simulating the reference ice shape. An inability of scaled shapes to simulate the reference shape is therefore evidence of a problem with either the  $MVD$  (affecting  $K_0$ ) or  $LWC$  (affecting  $A_c$ ) calibration of the cloud.

Figure 6 gives the reference and scale ice shapes for the rime case 73 tests for the Feo (fig. 6(a)), constant- $V$  (fig. 6(b)), constant- $We$  (fig. 6(c)) and average- $V$  (fig. 6(d)) methods of selecting scale velocity. The scale velocity required to satisfy constant- $Re$  was 219 m/s, well in excess of the IRT capability, so this method could not be tested for this case. Both the Feo and constant- $V$  methods produced scale shapes that matched the reference in shape and quantity. However, while the constant- $We$  and average- $V$  results simulated the reference shape, neither produced sufficient quantity of ice. It was suspected, therefore, that the  $MVD$ s for the results shown in figures 6(c) and (d) were properly scaled, but the scale  $LWC$  values were too low.

The target  $MVD$  and  $LWC$  values for these March 1998 tests were established by setting spray-bar air and water pressures according to a 1997 calibration of the IRT. The tunnel was recalibrated in November 1998<sup>12</sup> as part

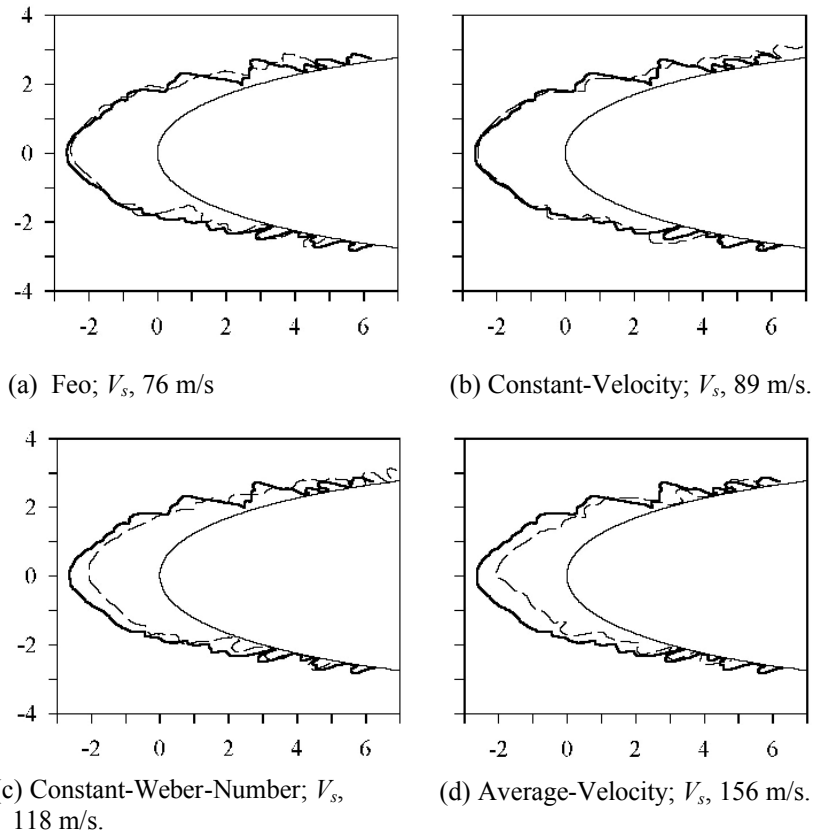


Figure 6. Scaling Results for Rime Ice Using Four Methods of Choosing Scale Velocity. Case 73 ( $n = 1.0$ ). Test Conditions in table II. Axes Units in cm. Scale Ice Shape Coordinates Doubled.

— Reference Shape,  $c_r$ , 53.3 cm;  $V_r$ , 90 m/s.  
 - - - Scale Shape;  $c_s$ , 27.7 cm;  $V_s$ , as indicated.

of an annual check. Slightly different procedures were used than in past calibrations, and the  $LWC$ s for given spray-bar pressures were found to be somewhat lower than for the 1997 calibrations. The greatest difference in  $LWC$  between the two calibrations was found at the highest velocities. When this new calibration was applied to the March data, the leading-edge thicknesses of these rime shapes correlated with the new accumulation parameter as shown in figure 7. Figure 7 includes data from the rime tests reported in figure 6 as well as from additional rime shapes that will not be presented here. Because the 1998 calibration appeared to explain the observed results with rime ice, it was used to determine the  $LWC$ s for the March 1998 tests as given in table II. This experience showed that a series of scaling tests performed with rime ice conditions can be an effective tool to check the consistency of icing tunnel cloud calibrations over a range of velocity.

The Mach number for the average- $V$  scaled conditions (fig. 6(d)) approached 0.5, well in excess of the compressible limit<sup>13</sup> of about 0.3. However, figure 6(d) does not indicate a scaled ice shape any different from

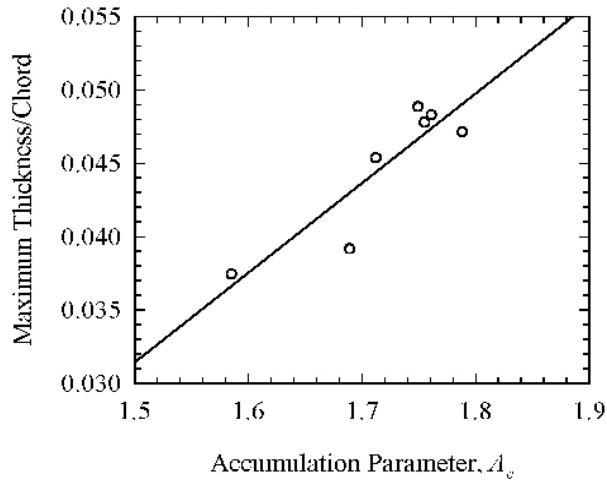


Figure 7. Correlation of Maximum Rime Ice Thickness with Accumulation Parameter,  $A_c$  Based on 1998 IRT Cloud Calibration.

that in figure 6(c) for which  $M = 0.37$ . This result and those to be given later suggest that compressibility probably has little effect on ice accretion, at least for  $M < .5$ .

#### Mixed Ice (Cases 110 and 111)

The case 110 ( $n = 0.8$ ) reference ice shape was mostly rime but with a narrow glaze region at the leading edge, as can be seen in figure 8. Due to time constraints, scaling tests for case 110 were made only with scale velocities from the Feo, constant- $V$  and constant- $We$  methods. Results are shown in figures 8(a), (b) and (c). For this icing condition, the quality of the scaled shape relative to the reference appeared to be independent of which of these three methods were used. All three scaled shapes, when coordinates were doubled, were

approximately the same size as the reference, but none exactly reproduced the leading-edge features.

Figure 9 presents the scaling results for case 111 ( $n = 0.7$ ). The reference shape for this case featured ice with small horns. A large feather structure immediately adjacent to the main shape grew into the side of the horns. For this case, scaling tests were only made with the constant- $We$ , average- $V$  and constant- $Re$  methods. None of the scaled ice shapes matched all the prominent features of the reference shape. The constant- $We$  and average- $V$  methods (figs. 9(a) and (b)) failed to reproduce the main horns although the large adjacent feathers were approximated.

The constant- $Re$ -scaled ice results are shown in figure 9(c). Although the scale Mach number for this test was 0.47, well above the maximum for incompressible flow, the scale ice shape simulated the reference shape in the region of the leading edge. However, the abundant feather growth of the reference ice was nearly non-existent in the scaled ice. It is possible that the high scale velocity prevented significant feather growth by causing fragile structures to shed.

#### Glaze Ice (Cases 112 and 113)

Case 112 had a freezing fraction of 0.5. The reference ice shape featured the horns typical of glaze ice with relatively small feathers farther back on the airfoil. All five scale-velocity methods were tested.

The Feo method (fig. 10(a)) produced scaled ice with a convex shape at the leading edge region. The resulting horns were somewhat farther back than the reference horns although the horn size was simulated well. As the scale velocity was increased by applying the constant- $V$  (fig. 10(b)) and constant- $We$  (fig. 10(c)) methods the horns moved farther forward. The lower

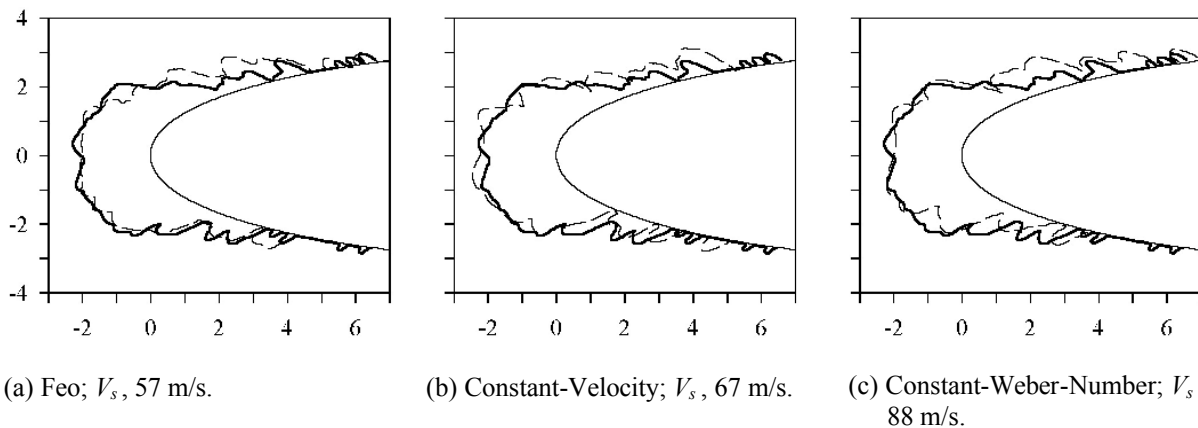


Figure 8. Scaling Results for Mixed Ice Using Three Methods of Choosing Scale Velocity. Case 110 ( $n = 0.8$ ). Test Conditions in table II. Axes Units in cm. Scale Ice Shape Coordinates Doubled.

— Reference Shape;  $c_r$ , 53.3 cm;  $V_r$ , 67 m/s.  
 - - - Scale Shape;  $c_s$ , 27.7 cm;  $V_s$ , as indicated.

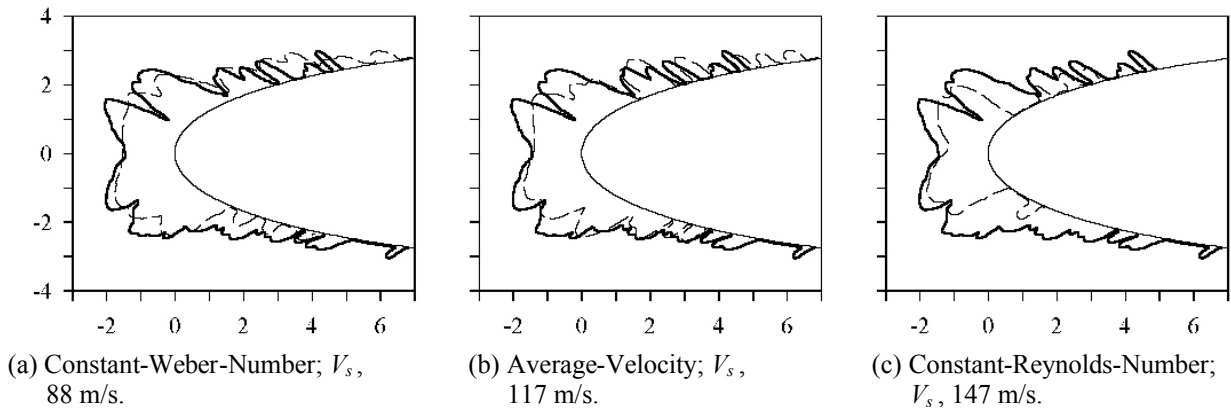


Figure 9. Scaling Results for Mixed Ice Using Three Methods of Choosing Scale Velocity. Case 111 ( $n = .7$ ). Test Conditions in table II. Axes Units in cm. Scale Ice Shape Coordinates Doubled.

—— Reference Shape,  $c_r$ , 53.3 cm;  $V_r$ , 67 m/s.  
 - - - - Scale Shape,  $c_s$ , 27.7 cm;  $V_s$ , as indicated.

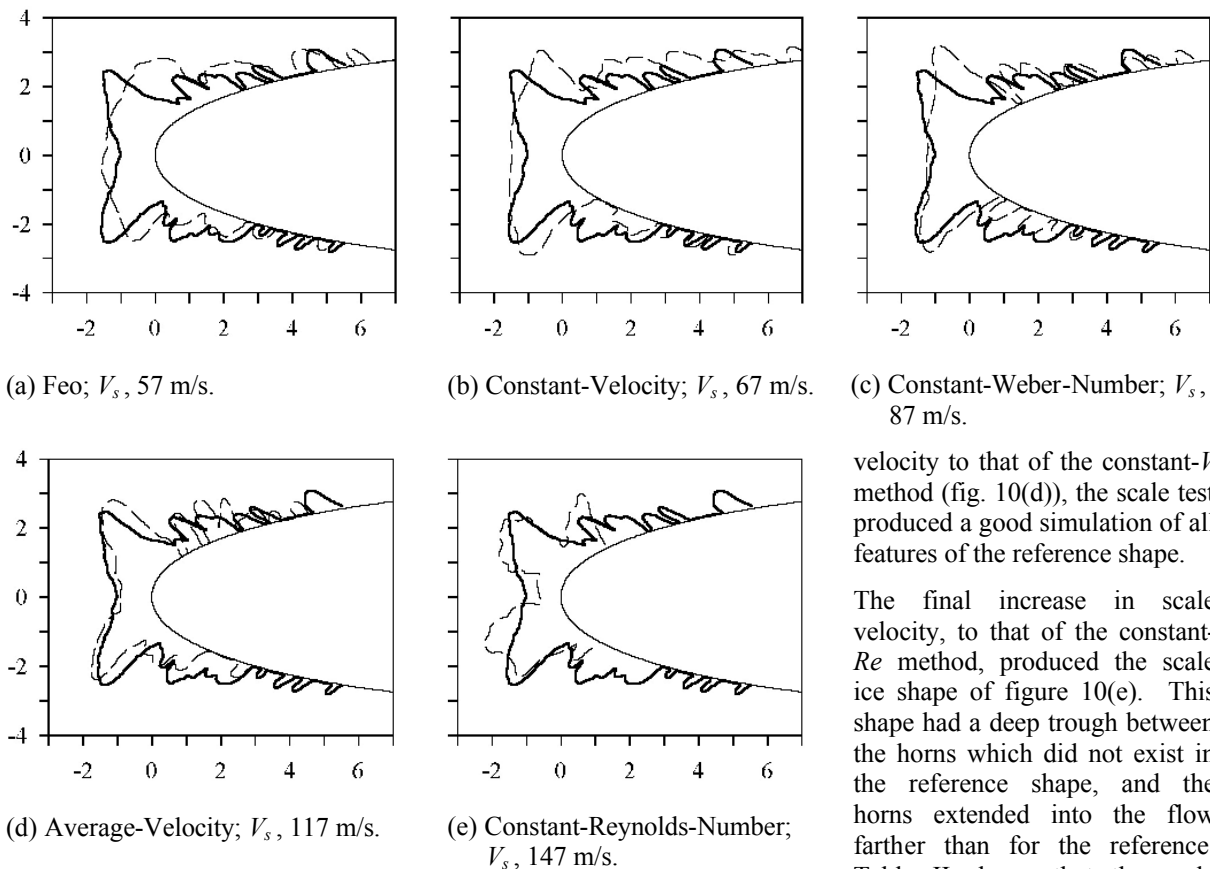


Figure 10. Scaling Results for Glaze Ice Using Five Methods of Choosing Scale Velocity. Case 112 ( $n = 0.5$ ). Test Conditions in table II. Axes Units in cm. Scale Ice Shape Coordinates Doubled.

—— Reference Shape,  $c_r$ , 53.3 cm;  $V_r$ , 67 m/s.  
 - - - - Scale Shape,  $c_s$ , 27.7 cm;  $V_s$ , as indicated.

horn of the constant- $We$  shape simulated the reference well, but the upper horn location was still somewhat aft of the reference. With a further increase in scale

velocity to that of the constant- $V$  method (fig. 10(d)), the scale test produced a good simulation of all features of the reference shape.

The final increase in scale velocity, to that of the constant- $Re$  method, produced the scale ice shape of figure 10(e). This shape had a deep trough between the horns which did not exist in the reference shape, and the horns extended into the flow farther than for the reference. Table II shows that the scale Mach number was in the compressible regime, but results cited previously suggested that  $M$  should have little significant effect on the leading-edge ice shape. The scale freezing fraction was about 10% lower than the reference, but probably more important, the total temperature was just

above the freezing temperature of water. This high temperature is probably the cause of the leading-edge distortion of the scaled shape.

In case 113 (fig. 11), the freezing fraction was 0.3. The reference ice shape was convex except for a small dip at the leading edge. The upper and lower horns grew nearly normal to the undisturbed airflow. Scaling results were obtained for the Feo, constant- $V$ , constant- $We$  and average- $V$  methods. The constant- $Re$  method

of case 112 (fig. 10(e)). Note from table II that the total temperatures of these two scale tests were nearly equal, a few tenths of a degree above freezing. The similarity of the features of these shapes along with the coincidentally high total temperatures support the supposition that these ice shapes were heavily influenced by the temperature.

### Concluding Remarks

To evaluate ways to choose scale velocity, a series of scaling tests were performed using the modified Ruff scaling method with 5 approaches to selecting scale velocity. Reference tests used a 53.3-cm-chord NACA 0012 model, and scale tests, a 27.7-cm-chord NACA 0012. Scale velocities ranged in value from 85% of the reference velocity (using a Feo constant-water-film thickness) to 220% (matching the scale  $Re$  to the reference.) The general conclusions from these tests can be summarized as follows:

1. A series of rime scaling tests using a range of scale velocities can be used to identify inconsistencies in tunnel cloud calibration.
2. For rime ice and ice formed with freezing fractions as low as 0.8, there appeared to be little effect of scale velocity on ice shape.
3. For ice formed with a freezing fraction of 0.7, limited evidence suggested that improved simulation of the reference shape at the leading edge may have been achieved as the scale velocity increased. However, for the scale tests using the constant- $Re$  approach, the feather structure was inadequate to simulate that of the reference ice shape. The high velocity of this test may have hindered feather development.
4. For ice formed with a freezing fraction of 0.5, improved simulation of the reference shape was achieved as the scale velocity increased, as long as scale total temperature did not exceed 0 °C.

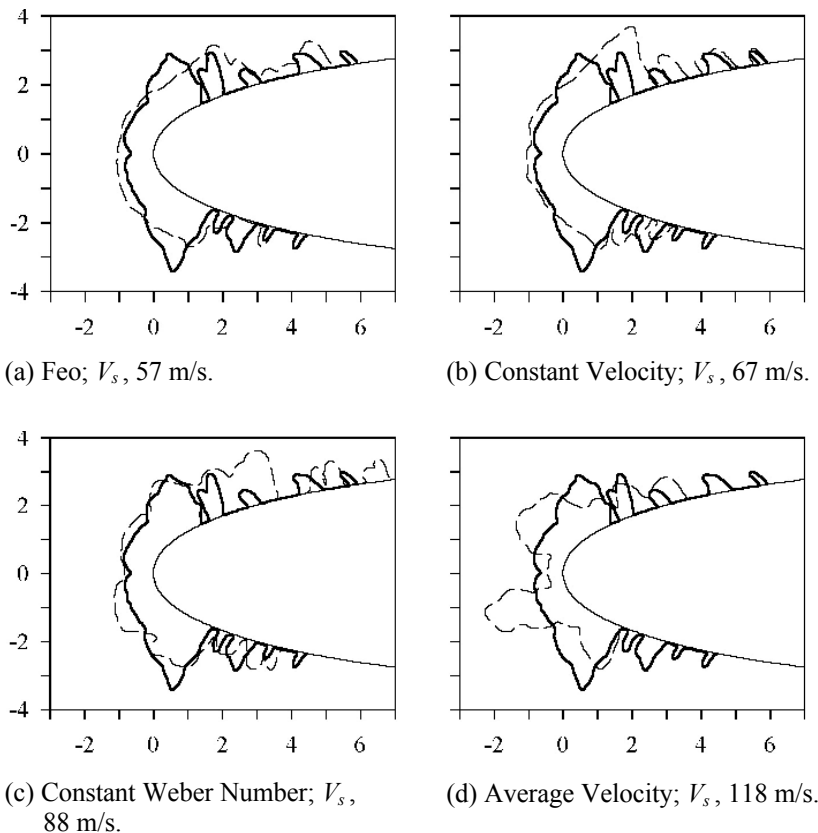


Figure 11. Scaling Results for Glaze Ice Using Four Methods of Choosing Scale Velocity. Case 113 ( $n = .3$ ). Test Conditions in table II. Axes Units in cm. Scale Ice Shape Coordinates Doubled.  
 ——— Reference Shape,  $c_r$ , 53.3 cm;  $V_r$ , 67 m/s.  
 - - - - Scale Shape,  $c_s$ , 27.7 cm;  $V_s$ , as indicated.

gave a scale total temperature of 3.2 °C; therefore, it was not tested. The scale shapes for the Feo (fig. 11(a)) and constant- $V$  (fig. 11(b)) methods were similar; both approximated the leading-edge region of the reference ice shape. However, the upper horns of the scale shapes were located too far back and the lower horns were smaller than the reference. The scaled shape for the constant- $We$  approach (fig. 11(c)) simulated the size and location of the upper horn well, but not the lower portion of the leading-edge region. The average- $V$  method (fig. 11(d)) produced a scaled shape with characteristics much like those of the constant- $Re$  test

5. At the lowest freezing fraction tested,  $n = 0.3$ , the scale velocity appeared to have little effect on the scaled ice shape, but few cases could be run without exceeding a total temperature of  $0^\circ\text{C}$ .
6. Tests in which the scale total temperature exceeded  $0^\circ\text{C}$  produced scaled ice shapes whose leading-edge features displayed no similarity to those of the reference shape, which had been formed at a lower temperature.
7. Mach numbers as high as 0.5 appeared to have no effect on the main ice shape.

The conclusions presented here are tentative. To insure the validity of the ice shapes on which they are based, the tests need to be repeated utilizing the most recent IRT cloud calibration.

Neither the Feo constant-water-film-thickness nor the constant- $We$  approach to choosing the scale velocity appeared to provide consistently better scaling than other methods tested. This result suggests that if the physics of surface water films is important to determining glaze ice shapes, neither of these methods adequately captures that physics.

Some of the results of this study may point to the importance of  $Re$  in scaling.  $Re$  has generally been neglected because attempts to match the scale and reference  $Re$  often result in scale velocities or temperatures that are excessive. Practical scaling methods often require compromises, but these can best be applied only after the most important parameters have been identified. Further evaluation of constant- $Re$  scaling is therefore encouraged.

Further study of the heat-transfer terms  $n$ ,  $\phi$ , and  $\theta$  may also be warranted, with the objective of determining if the expressions for these parameters properly describe the physics of ice accretion.

#### References

1. Langmuir, Irving and Blodgett, Katharine B.: "A Mathematical Investigation of Water Droplet Trajectories," Army Air Forces Technical Report No. 5418, February 1946.
2. Messinger, B.L., "Equilibrium Temperature of an Unheated Icing Surface as a Function of Airspeed," J. Aeron. Sci. 20 No. 1, Jan. 1953, pp. 29–42.

3. Ruff, G.A.: "Analysis and Verification of the Icing Scaling Equations," AEDC–TR–85–30, Vol. 1 (Rev), March 1986.
4. Anderson, David N., "Methods for Scaling Icing Test Conditions," AIAA–95–0540 and NASA TM–106827, January 1995.
5. Olsen, W. and Walker, E., "Experimental Evidence for Modifying the Current Physical Model for Ice Accretion on Aircraft Surfaces," NASA TM–87184, 1986.
6. Bilanin, A. J., "Proposed Modifications to the Ice Accretion/Icing Scaling Theory," AIAA Paper AIAA–88–0203, January 1988.
7. Bilanin, Alan J. and Anderson, David N.: "Ice Accretion with Varying Surface Tension," AIAA–95–0538 and NASA TM–106826, January 1995.
8. Anderson, David N., "Evaluation of Constant-Weber-Number Scaling for Icing Tests," AIAA–96–0636 and NASA TM–107141, January 1996.
9. Feo, Alejandro, INTA, personal communication, 1997.
10. Feo, A. and Urdiales, M., "Stagnation Point Probe in a Water Spray Immersed in an Airstream,"  $\phi$ AE/TNO/0452/003/INTA/95, Instituto Nacional de Técnica Aeroespacial, February 1995.
11. Soeder, Ronald H., Sheldon, David W., Andracchio, Charles R., Ide, Robert F., Spera, David A. and Lalli, Nick M., "NASA Lewis Icing Research Tunnel User Manual," NASA TM–107159, June 1996.
12. Ide, Robert F., "Operating Envelopes and Calculation Procedure for Spray Settings for the NASA-Lewis Icing Research Tunnel," unpublished NASA Lewis document, November 1998.
13. Schlichting, Hermann, *Boundary Layer Theory*, McGraw-Hill, New York, 1960, p. 9.

Table II. Average Test Conditions with Corresponding Parameter Values

Case	Type	Date/Run	$c$ , cm	$t_{sb}$ , °C	$t_{tot}$ , °C	$V$ , m/s	$MTD$ , $\mu\text{m}$	$LWC$ , $\text{g}/\text{m}^3$	$\tau$ , min	$P_{vis}$ , $10^5$ $\text{nt}/\text{m}^2$	$P_{tot2}$ , $10^5$ $\text{nt}/\text{m}^2$	$K_0$	$A_c$	$n$	$b$	$\phi$ , °C	$\theta$ , °C	$Re$ , $10^4$	$We$ , $10^3$	$M$
73	Ref	3-27-98/6	53.3	-20.6	-16.6	89.5	40.0	0.51	10.0	0.93	0.98	6.97	1.76	1.00	0.36	1.8	8.3	12.2	4.93	0.28
73	Feo	3-18-98/7	26.7	-20.2	-17.3	76.3	28.0	0.81	3.7	0.94	0.98	7.14	1.79	1.00	0.37	1.7	8.7	5.26	2.50	0.24
73	Const $V$	3-19-98/9	26.7	-20.5	-16.5	89.4	25.5	0.72	3.5	0.93	0.98	6.81	1.75	1.00	0.35	1.8	8.2	6.09	3.13	0.28
73	Const $We$	3-20-98/9	26.7	-21.2	-14.3	117.8	23.2	0.56	3.3	0.89	0.97	7.01	1.69	1.00	0.32	1.8	6.9	7.77	4.95	0.37
73	Avg $V$	3-23-98/11	26.7	-22.4	-10.3	155.9	21.0	0.40	3.3	0.85	0.99	7.25	1.59	1.00	0.27	1.8	4.3	9.72	7.85	0.49
110	Ref	3-27-98/5	53.3	-13.9	-11.6	67.3	40.0	0.61	11.2	0.95	0.98	5.85	1.79	0.83	0.36	-4.5	1.3	8.98	2.78	0.21
110	Feo	3-18-98/6	26.7	-13.7	-12.1	56.9	27.0	0.96	4.2	0.96	0.98	5.59	1.80	0.83	0.37	-4.4	1.6	3.83	1.35	0.18
110	Const $V$	3-19-98/8	26.7	-13.9	-11.7	67.1	26.2	0.86	4.0	0.95	0.98	5.91	1.79	0.83	0.36	-4.4	1.4	4.48	1.81	0.21
110	Const $We$	3-20-98/8	26.7	-14.2	-10.4	87.6	23.5	0.68	3.6	0.93	0.97	5.89	1.69	0.87	0.33	-4.5	0.5	5.74	2.77	0.27
111	Ref	3-26-98/6	53.3	-11.1	-8.9	67.1	40.0	0.61	11.2	0.96	0.99	5.84	1.78	0.67	0.37	-7.2	-2.4	8.79	2.77	0.21
111	Const $We$	3-23-98/9	26.7	-11.5	-7.6	87.8	23.5	0.68	3.7	0.94	0.99	5.89	1.71	0.69	0.33	-7.2	-3.2	5.65	2.78	0.27
111	Avg $V$	3-23-98/8	26.7	-12.3	-5.4	117.4	20.8	0.50	3.6	0.91	0.99	5.87	1.63	0.72	0.29	-7.1	-4.4	7.31	4.41	0.36
111	Const $Re$	3-23-98/4	26.7	-13.2	-2.3	147.4	19.0	0.39	3.8	0.86	0.99	5.94	1.70	0.69	0.26	-7.2	-6.4	8.80	6.35	0.46
112	Ref	3-26-98/4	53.3	-8.4	-6.1	67.0	40.0	0.61	11.2	0.96	0.98	5.83	1.78	0.49	0.37	-10.0	-6.3	8.62	2.76	0.21
112	Feo	3-18-98/3	26.7	-8.2	-6.5	56.9	27.0	0.96	4.2	0.96	0.98	5.57	1.78	0.49	0.38	-10.0	-6.1	3.68	1.34	0.17
112	Const $V$	3-19-98/6	26.7	-8.4	-6.1	67.2	26.2	0.86	4.0	0.95	0.98	5.90	1.79	0.49	0.37	-10.0	-6.3	4.32	1.82	0.21
112	Const $We$	3-19-98/4	26.7	-8.6	-4.8	87.4	23.5	0.68	3.7	0.93	0.98	5.87	1.74	0.50	0.34	-10.1	-7.2	5.52	2.76	0.27
112	Avg $V$	3-20-98/2	26.7	-9.5	-2.6	117.4	20.8	0.50	3.8	0.89	0.98	5.87	1.72	0.51	0.29	-9.9	-8.4	7.18	4.41	0.36
112	Const $Re$	3-23-98/1	26.7	-10.2	0.5	146.8	19.0	0.39	4.3	0.86	0.99	5.91	1.91	0.45	0.26	-10.1	-10.4	8.62	6.30	0.45
113	Ref	3-26-98/2	53.3	-5.5	-3.3	67.1	40.0	0.61	11.2	0.96	0.99	5.83	1.78	0.31	0.37	-12.8	-10.5	8.48	2.77	0.20
113	Feo	3-18-98/2	26.7	-5.5	-3.8	57.0	27.5	0.96	4.1	0.96	0.98	5.74	1.76	0.32	0.38	-12.7	-10.1	3.63	1.37	0.17
113	Const $V$	3-19-98/3	26.7	-5.7	-3.4	67.1	26.2	0.86	4.0	0.95	0.98	5.90	1.79	0.32	0.37	-12.7	-10.4	4.24	1.82	0.20
113	Const $We$	3-19-98/1	26.7	-5.9	-2.1	87.8	23.5	0.68	3.9	0.93	0.98	5.88	1.81	0.31	0.34	-12.8	-11.2	5.45	2.78	0.27
113	Avg $V$	3-23-98/2	26.7	-6.7	0.2	117.8	20.8	0.49	4.3	0.90	0.98	5.87	1.97	0.29	0.29	-12.7	-12.6	7.08	4.44	0.36

<b>REPORT DOCUMENTATION PAGE</b>			<i>Form Approved</i> <i>OMB No. 0704-0188</i>	
Public reporting burden for this collection of information is estimated to average 1 hour per response, including the time for reviewing instructions, searching existing data sources, gathering and maintaining the data needed, and completing and reviewing the collection of information. Send comments regarding this burden estimate or any other aspect of this collection of information, including suggestions for reducing this burden, to Washington Headquarters Services, Directorate for Information Operations and Reports, 1215 Jefferson Davis Highway, Suite 1204, Arlington, VA 22202-4302, and to the Office of Management and Budget, Paperwork Reduction Project (0704-0188), Washington, DC 20503.				
<b>1. AGENCY USE ONLY (Leave blank)</b>		<b>2. REPORT DATE</b> June 2003	<b>3. REPORT TYPE AND DATES COVERED</b> Final Contractor Report	
<b>4. TITLE AND SUBTITLE</b>  Evaluation of Methods to Select Scale Velocities in Icing Scaling Tests			<b>5. FUNDING NUMBERS</b>  WU-708-20-13-00 NCC3-884	
<b>6. AUTHOR(S)</b>  David N. Anderson and Gary A. Ruff				
<b>7. PERFORMING ORGANIZATION NAME(S) AND ADDRESS(ES)</b>  Ohio Aerospace Institute 22800 Cedar Point Road Brook Park, Ohio 44142			<b>8. PERFORMING ORGANIZATION REPORT NUMBER</b>  E-13520	
<b>9. SPONSORING/MONITORING AGENCY NAME(S) AND ADDRESS(ES)</b>  National Aeronautics and Space Administration Washington, DC 20546-0001			<b>10. SPONSORING/MONITORING AGENCY REPORT NUMBER</b>  NASA CR-2003-211827 AIAA-99-0244	
<b>11. SUPPLEMENTARY NOTES</b>  Prepared for the 37th Aerospace Sciences Meeting and Exhibit sponsored by the American Institute of Aeronautics and Astronautics, Reno, Nevada, January 11-14, 1999. David N. Anderson, Ohio Aerospace Institute, Brook Park, Ohio, and Gary A. Ruff, Drexel University, Philadelphia, Pennsylvania. Project Manager, Thomas H. Bond, Turbomachinery and Propulsion Systems Division, NASA Glenn Research Center, organization code 5840, 216-433-3900.				
<b>12a. DISTRIBUTION/AVAILABILITY STATEMENT</b>  Unclassified - Unlimited Subject Category: 02 Available electronically at <a href="http://gltrs.grc.nasa.gov">http://gltrs.grc.nasa.gov</a> This publication is available from the NASA Center for AeroSpace Information, 301-621-0390.			<b>12b. DISTRIBUTION CODE</b>	
<b>13. ABSTRACT (Maximum 200 words)</b>  A series of tests were made in the NASA Glenn Icing Research Tunnel to determine how icing scaling results were affected by the choice of scale velocity. Reference tests were performed with a 53.3-cm-chord NACA 0012 airfoil model, while scale tests used a 27.7-cm-chord 0012 model. Tests were made with rime, mixed, and glaze ice. Reference test conditions included airspeeds of 67 and 89 m/s, an <i>MVD</i> of 40 $\mu\text{m}$ , and <i>LWCs</i> of 0.5 and 0.6 $\text{g}/\text{m}^3$ . Scale test conditions were established by the modified Ruff (AEDC) scaling method with the scale velocity determined in five ways. The resulting scale velocities ranged from 85 to 220 percent of the reference velocity. This paper presents the ice shapes that resulted from those scale tests and compares them to the reference shapes. It was concluded that for freezing fractions greater than 0.8 as well as for a freezing fraction of 0.3, the value of the scale velocity had no effect on how well the scale ice shape simulated the reference shape. For freezing fractions of 0.5 and 0.7, the simulation of the reference shape appeared to improve as the scale velocity increased.				
<b>14. SUBJECT TERMS</b>  Aircraft safety; Aircraft icing; Scaling			<b>15. NUMBER OF PAGES</b> 17	
			<b>16. PRICE CODE</b>	
<b>17. SECURITY CLASSIFICATION OF REPORT</b> Unclassified	<b>18. SECURITY CLASSIFICATION OF THIS PAGE</b> Unclassified	<b>19. SECURITY CLASSIFICATION OF ABSTRACT</b> Unclassified	<b>20. LIMITATION OF ABSTRACT</b>	